ORIGINAL PAPER

Comparative Adsorption of Cd (II) and Pb (II) by MCM-48 and Amine-Grafted MCM-48 in Single and Binary Component Systems

Hadi Vatandoust[1] · Habibollah Younesi[1] · Zahra Mehraban[2] · Ava Heidari[3] · Hussein Khakpour[4]

Abstract

MCM-48 were prepared using hexadecyl trimethyl ammonium bromide and TEOS and modified with N^1-(3-trimethoxysilylpropyl) diethylenetriamine by post-synthesis method to develop efficient adsorbent for heavy metal adsorption. These materials were determined by X-ray diffraction, N_2 adsorption–desorption measurement, and scanning electron microscopy. The results show that the modification of MCM-48 resulted in a decrease in the Brunauer–Emmett–Teller surface area and total pore volume. Batch adsorption technique in the single and multicomponent systems was used in this study. The experimental parameters' influence was investigated, and the results indicated that amine-attached MCM-48 indicated higher adsorption efficiency for metal ions than MCM-48. Langmuir and Freundlich models modeled the equilibrium data in a single system, whereas two-component data fitted to the extended Langmuir model. The maximum adsorption capacity (q_m, single system) of NH_2-NH-NH-MCM-48 for cadmium and lead was 82.7 and 119.24 mg g^{-1}, respectively. In both adsorption systems, the affinity of NH_2-NH-NH-MCM-48 for cadmium was more significant than that for lead.

Keywords Heavy metal · Removal · Mesoporous silica · Surface modification

Introduction

Heavy metal contamination has turned into one of the most significant environmental issues today, because they are poisonous and carcinogenic and, even in low concentration, can accumulate throughout the food chain [1–3]. Lead and cadmium are dangerous heavy metals. Several techniques for heavy metal elimination from wastewater are available such as filtration [4], reverse osmosis [5], coagulation-flocculation, ion exchange [6], precipitation [7], and adsorption [8–11]. Adsorption has developed one of the few promising methods for treating industrial wastewater, especially using efficient adsorbent.

Mesoporous silica materials can be used in the field of the environment due to the high surface area, specific structure, narrow pore size distribution, homogeneous pore size, and biocompatibility [11–15]. Surface functionalization of ordered mesoporous silica with different functional groups such as –NH_2, -SH, -S-, and SO_3H has been reported by researchers to acquire large adsorption capacity. For example, Heidari et al. developed the amino-functionalized MCM-41 for the removal of Ni (II), Cd (II), and Pb (II) ions from aqueous solution and found the highest maximum adsorption capacity of 57.74 mg/g for Pb (II). Han et al. [16] prepared aminopropyl-functionalized MCM-48 by co-condensation for the adsorption of bivalent metal irons from a single-component system. Their results indicated the highest adsorption capacity for Pb (II) compared to others (Mn (II), Ni (II), Cu (II), and Cd (II)). Benhamou et al. [17] modified the surface of MCM-48 by post-synthesis method with N–N dimethyldodecylamine and dodecylamine and used them for adsorption of heavy metal in aqueous solution. They found that the adsorption capacity order for metal ions was Cu (II) > Pb (II) > Cd (II) > Co (II). Ebrahimzadeh et al. [18]

✉ Ava Heidari
heidari@um.ac.ir

1 Department of Environmental Science, Faculty of Natural Resources and Marine Sciences, Tarbiat Modares University, P.O. Box 46414-356, Noor, Iran

2 Research Institution for Curriculum Development and Educational Innovations, New Technologies Committee, 1584634818 Tehran, Iran

3 Department of Environmental Science, Faculty of Natural Resources and Environment, Ferdowsi University of Mashhad, Mashhad, Iran

4 Chemical Engineering Department, Faculty of Engineering, Shomal University, PO Box 731, Amol, Mazandaran, Iran

grafted aminopropyl on the surface MCM-48 using the post-synthesis method and evaluated its capability for Au (III) and Pd (II). The obtained adsorption capacity of Au (III) and Pd (II) was 305 and 153 mg/g. In the above studies, different types of silanes and polymers containing amine groups have been used for the functionalization of MCM-48. Their findings displayed that the number of amine groups and the pathway of functionalization (post-synthesis or co-condensation) affects the adsorption capacity. However, there is still a need for the introduction of various amine groups onto MCM-48 to enhance its adsorption capacity and selectivity towards heavy metals. Herein, we focused on designing the Pb (II) and Cd (II) ions selective aminosilane-grafted adsorbent. Synthesis and characterization of modified mesoporous silica MCM-48 using N1-(3-trimethoxysilylpropyl) diethylenetriamine and its application in single and binary component systems were investigated for the first time.

In this study, MCM-48 was synthesized and functionalized, and used for comparative adsorption of Cd (II) and Pb (II) ions from aqueous solution in a single and multicomponent system study. The influence of various adsorption conditions on the removal performance of Cd (II) and Pb (II) actions was examined.

Materials and Methods

Materials

In this study, hexadecyl trimethyl ammonium bromide, n-hexane, toluene, and hydrochloric acid (37%) from Merck Co.; sodium hydroxide, tetraethoxysilane 98%, and N^1-(3-trimethoxysilylpropyl) diethylene triamine from Sigma-Aldrich Co; and CdCl$_2$ and Pb(NO$_3$)$_2$ from Sigma-Aldrich Co were purchased.

Synthesis of MCM-48

MCM-48 was prepared based on the method of Wang et al. [19]. The source of silica was tetraethoxysilane, and hexadecyl trimethyl ammonium bromide was used as a surfactant. Typically, 10 mL of TEOS was added to 50 mL of deionized water. The above mixture was agitated and heated at 35 °C for 40 min. Then, 0.6 g of NaOH was added to the mixture under the string. After 1 h agitated at 35 °C, 10.61 g of CTAB was added to the gel under agitation for 1 h at 110 °C. Then, the resulting homogenous mixture was transferred into a bottle and inserted into the oven at 120 °C for 24 h and the crystallization was performed. After that, the obtained material was filtered and washed with deionized water several times. The synthesized MCM-48 was dried at room temperature and then calcined for 6 h at 550 °C with a heating rate of 2 °C/min.

Synthesis of Amine-Functionalized MCM-48

The amine-functionalized MCM-48 (NH$_2$-NH-NH-MCM-48) was synthesized based on the procedure of Yokoi et al. [20]. Briefly, 0.5 g of calcined MCM-48 was suspended in 100 mL of the dry toluene and stirred for 30 min, and then 1 mL of N^1-(3-trimethoxysilylpropyl) diethylene triamine (modifying agent) was added to the mixture and refluxed for 8 h at 60 °C. The obtained material was washed with n-hexane and toluene several times, dried, and stored in a desiccator.

Characterization

X-ray diffraction (XRD) patterns of MCM-48 and NH$_2$-NH-NH-MCM-48 were attained using an XRD diffractometer (X'pert, Phillips, and Holland). Nitrogen adsorption–desorption isotherms of the adsorbents were measured at 77 K using a Micromeritics Instrument Model ASAP 2010. The surface shape of MCM-48 was observed by scanning electron microscopy (SEM, Phillips XL30, and Holland).

Adsorption Experiments

The batch process was employed onto the MCM-48 and NH$_2$-NH-NH-MCM-48 at room temperature in single and binary systems. All experiments were done in triplicate. A stock solution of cadmium and lead (1000 mg L^{-1}) ions was prepared by dissolving a proper amount of Pb(NO$_3$) and Cd(Cl)$_2$ in deionized water. For each experiment, 100 mL of the aqueous solution of these metals in different concentrations was placed in 250-mL Erlenmeyer flasks. During the adsorption process, the samples were got at different time intervals; the supernatant was filtered with 0.45-μm filter paper (Whatman) to ensure that mesoporous particles were removed. The concentration of cadmium and lead ions in the supernatant remaining was measured by atomic absorption spectroscopy. The pH of the metal ion aqueous solution was adjusted to 6 by adding NaOH and HCl (0.1 M). The removal efficiency (%) and the adsorption capacity (mg g^{-1}) were considered by the following calculations:

$$R = \frac{C_0 - C_e}{C_0} \times 100 \qquad (1)$$

$$qe = \frac{(C_0 - C_e)V}{m} \qquad (2)$$

where R (%) is the metal removal percentage, C_0 (mg L^{-1}) is the initial metal concentration, C_e (mg L^{-1}) is the equilibrium metal concentration, q_e (mg g^{-1}) is the equilibrium

adsorption capacity of adsorbent, V (L) is the volume of solution, and m (g) is the quantity of the adsorbent.

Equilibrium and Adsorption Studies

Adsorption Isotherms

The Langmuir and Freundlich models are the most usual types of models which wildly used to describe the adsorption of metal ions by adsorbents. Langmuir equation model can be expressed by [19, 21]:

$$q_e = \frac{q_m K_L C_e}{1 + K_L C_e} \qquad (3)$$

where q_e (mg g^{-1}) is the equilibrium adsorption capacity, C_e (mg L^{-1}) is the equilibrium metal concentration, q_m (mg g^{-1}) is the maximum adsorption capacity, and K_L (mg L^{-1}) is constant associated with the adsorption bonding energy. Freundlich model is given by:

$$q_e = K_F C_e^{1/n} \qquad (4)$$

where K_F (mg L^{-1}) and $1/n$ are the Freundlich coefficients indicative of the relative adsorption capacity and the intensity of adsorption.

The Langmuir competitive model (LCM) is an extended configuration of the Langmuir model to evaluate the experimental binary adsorption data of lead and cadmium. The CML isotherm equation is given as follows [22–26]:

$$Q = \frac{K_{L1} q_m C_{e1}}{1 + K_{L1} C_{e1} + C_{e2} K_{L2}} \qquad (5)$$

where K_{L1} and K_{L2} (L mg^{-1}) are the constants depicted by fitting the Langmuir model to the single-component adsorption data.

Adsorption Kinetics

The pseudo-first-order kinetic and the pseudo-second-order kinetic models are given by [27–29]:

$$\log\left(q_e - q_t\right) = \log q_e - \frac{K_1}{2.303} \qquad (6)$$

$$\frac{t}{q_t} = \frac{1}{K_2 q_e^2} + \frac{t}{q_e} \qquad (7)$$

where q_e and q_t (mg g^{-1}) are the equilibrium adsorption capacity and adsorption capacity at t time, and K_1 and K_2 (1/min) are the rate constants of pseudo-first-order and pseudo-second-order, respectively. The q_e, K_1, and K_2 were calculated from the slope and the intercept of plots of Eqs. 6 and 7.

Desorption and Regeneration

Desorption and regeneration experiments were carried out using MCM-48 and NH$_2$-NH-NH-MCM-48 adsorbents at the batch process, separately. After the adsorption experiment, the adsorbent was separated from the solution by centrifugation and subsequently washed with distilled water, dried in the oven at 60 °C, and weighted. Then, it was suspended in 100 mL of 1 M HNO$_3$ solution desorption agent. The mixture was agitated for 120 min and centrifuged. The concentration of metal ions was measured. For reuse of the spent adsorbent after adsorption, the residue sludge from the desorption study was washed, dried, and weighed. Then, it is used for adsorption experiments. The adsorption study of cadmium and lead onto these adsorbents followed conditions: initial metal concentration of 10 mg L^{-1}, the adsorbent quantity of 0.5 g L^{-1}, pH of 5, string speed of 200 rpm, room temperature, and reaction for 20 min. The detailed adsorption procedures were described in the "Adsorption Experiments" section. The adsorption–desorption cycles of the adsorbents were repeated five times under the same condition. The adsorption recovery was calculated by [30]:

Desorption recovery

$$= \frac{Quantity\ of\ metal\ desorbed\ to\ elution\ medium}{Quantity\ of\ metal\ adsorbed\ on\ adsorbent}$$

$$\times 100 \qquad (8)$$

Results and Discussions

Characterization of Adsorbents

Figure 1 shows the XRD spectra of MCM-48. The XRD pattern of MCM-48 displays a strong (211) peak and proportional (220) peak at the low angle region of $2\theta = 3.2$–$3.55°$, indicating the cubic phase of MCM-48 materials. Several other diffraction peaks with lower intensities are shown in the high angle region of $2\theta = 4$–$6°$, which can be indexed (321), (400), (420), (322), (422), (431), (611), and (543) diffraction peaks. These findings indicate the presence of a highly ordered cubic pore in the structure of MCM-48.

The adsorption–desorption isotherms of nitrogen at 77 K on MCM-48 and amine-grafted MCM-48 were investigated (figure not shown). The MCM-48 isotherm presents a type IV profile based on IUPAC classification with H1 hysteresis loops, which indicated mesoporous material, while after the

Fig. 1 SEM image, XRD pattern, FTIR spectra, and N_2 adsorption–desorption isotherms of MCM-48 (**a**) and NH_2-NH-NH-MCM-48 (**b**)
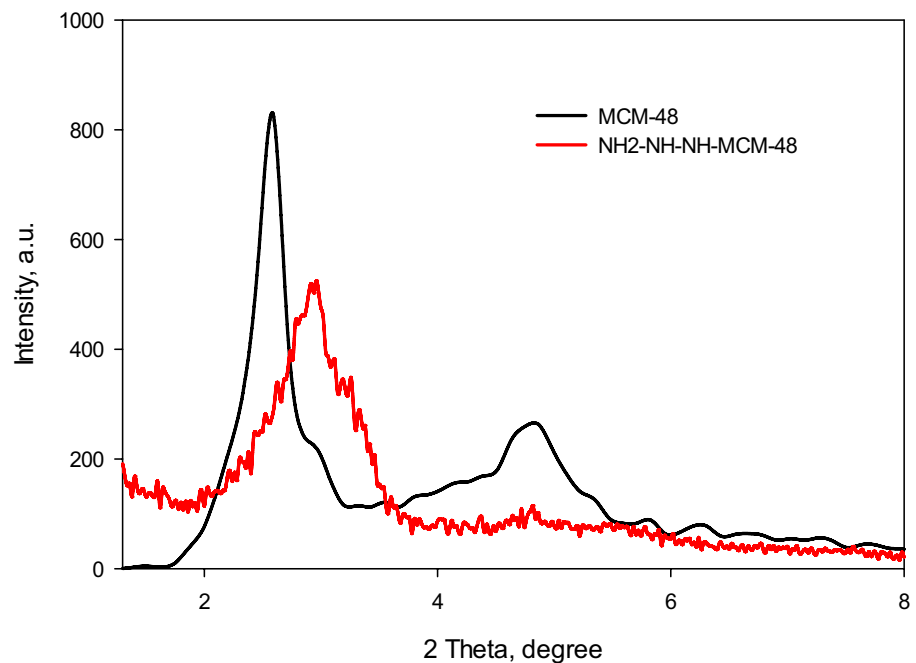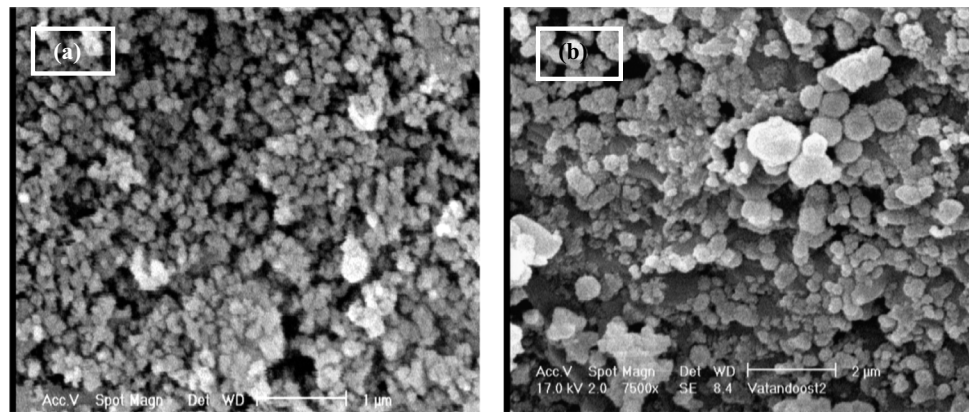
modification with an amine group (NH2-NH-NH-MCM-48 adsorbent) illustrated the type I isotherm, which is typical of microporous solids (Fig. 1). The Brunauer–Emmett–Teller (BET) surface area, pore volume, and the average pore size of these adsorbents were determined. The surface area of MCM-48 and total pore volume decreased from 1062 to 736 m^2/g and from 1.743 to 0.343 cm^3/g, respectively, after grafting with the functional ligand. This is most likely because of the set down of the amine-functionalized groups on the adsorbents' pores [31]. The SEM image of MCM-48 is illustrated in Fig. 1. As presented in Fig. 1, MCM-48 typically has a sphere-like shape.

Figure 1 displays the FTIR spectra of MCM-48 and NH_2-NH-NH-MCM-48 in the 400–4000 cm^{-1} region. The absorption bands at 463 and 802 cm^{-1} are related to the asymmetric and symmetric vibration of the Si–O-Si band [32, 33]. The band that appeared at 1080 cm^{-1} was also the Si–O-Si band [32, 33]. Broadband in 3449 and 3417 cm^{-1}

is ascribed to the stretching band of Si–O–H [34]. The week peak located at 1636 cm^{-1} attributed to the bending vibration of adsorbed water molecules [17]. Compared to the MCM-48, the NH_2-NH-NH-MCM-48 shows the peaks at 2916 and 2847 cm^{-1} related to the CH_2 stretching modes [17, 35]. Also, the absorption band at 1543 cm^{-1} corresponded to the NH_2 bending [35]. It confirmed that the amine groups incorporated silica structure through functionalization successfully.

Adsorption Study

Effect of Adsorbent Dose

The effect of different quantities of MCM-48 and NH_2-NH-NH-MCM-48 (0.125, 0.5, 1.25, 2.5, 5, 7.5, and 10 g L^{-1}) on the adsorption of Cd (II) and Pb (II) metal ions was studied. The experiments were carried out at pH

Fig. 1 (continued)
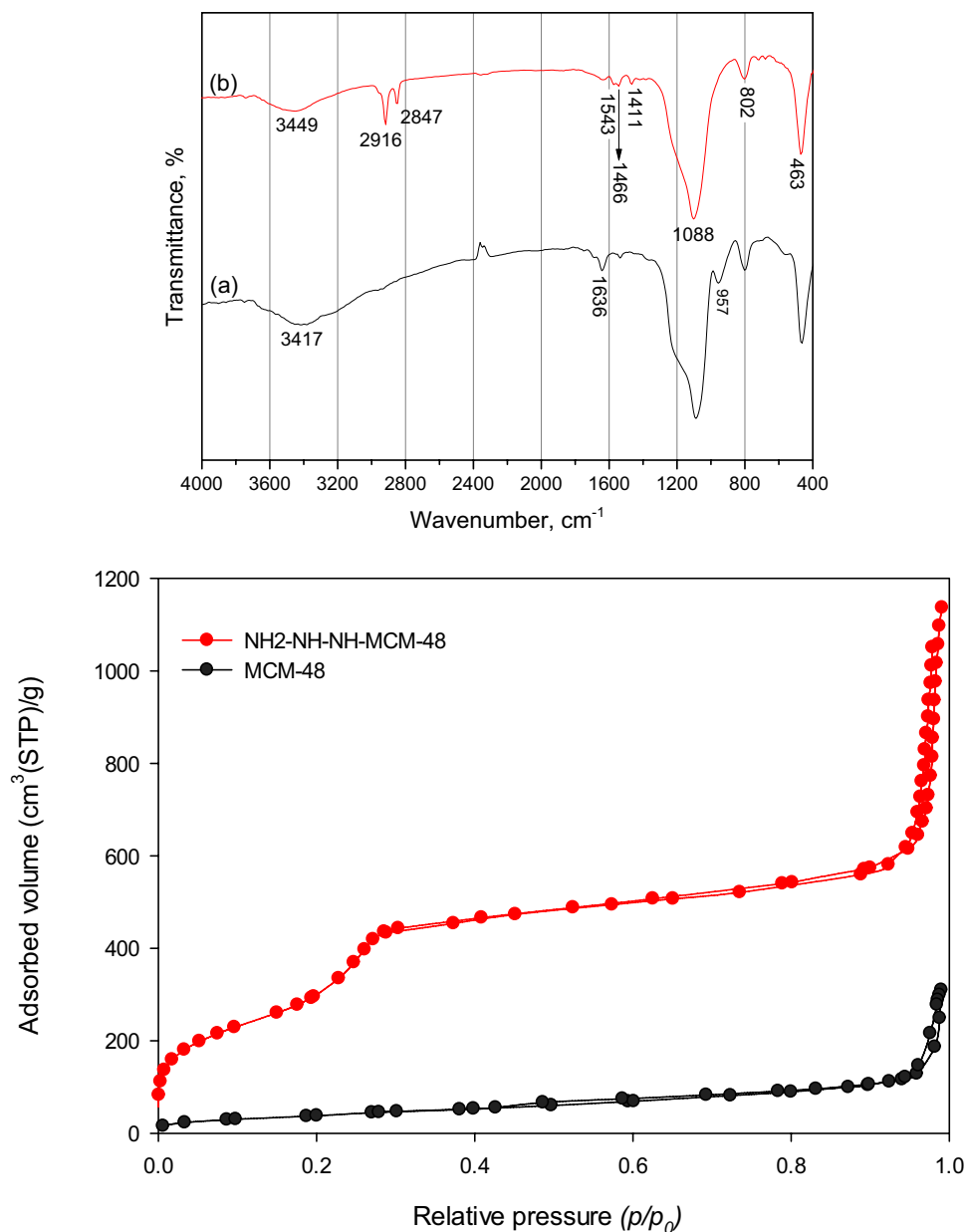
6, contact time of 120 min, the initial metal concentration of 50 mg L^{-1}, and room temperature. Their results were shown in Fig. 2. As seen in this figure, the percentage removal of metal ions increased significantly with an increase in both adsorbent dosages from 0.125 to 5 g L^{-1} and tended to reach a saturation level in the range of 5 to 10 g L^{-1}. Furthermore, for both adsorbents and both metal ions, the increment in adsorption capacity, q_e, was depicted with an increase in adsorbent dosage (Fig. 2). This can be explained by an increment in BET surface area, which leads to the accessibility of different binding sites for adsorption [36]. It is known that the maximum metal ions removal was obtained at about 10 g L^{-1} of MCM-48 and NH$_2$-NH-NH-MCM-48. As shown in Fig. 2a

and b, 10 g L^{-1} of MCM-48 and NH$_2$-NH-NH-MCM-48 removes 37 and 95% of Cd (II) and 34 and 88.5% of Pb (II), respectively. In the experiments, an adsorbent dose of 0.5 g L^{-1} of MCM-48 and NH$_2$-NH-NH-MCM-48 was used.

Effect of the pH

To investigate the influence of the pH on the adsorption of cadmium and lead ions by MCM-48 and NH$_2$-NH-NH-MCM-48, adsorption experiments were conducted in a pH range of 2 to 6, keeping all other parameters constant (the adsorbent dose of 0.5 g L^{-1}, the initial metal concentration of 10 mg L^{-1}, and contact time 2 h). This
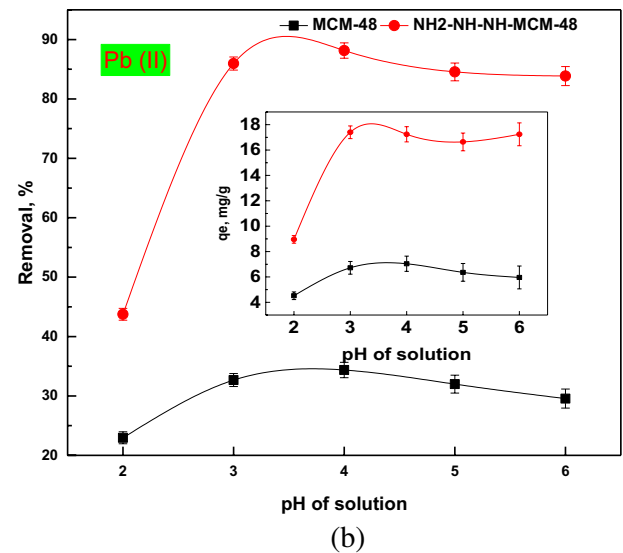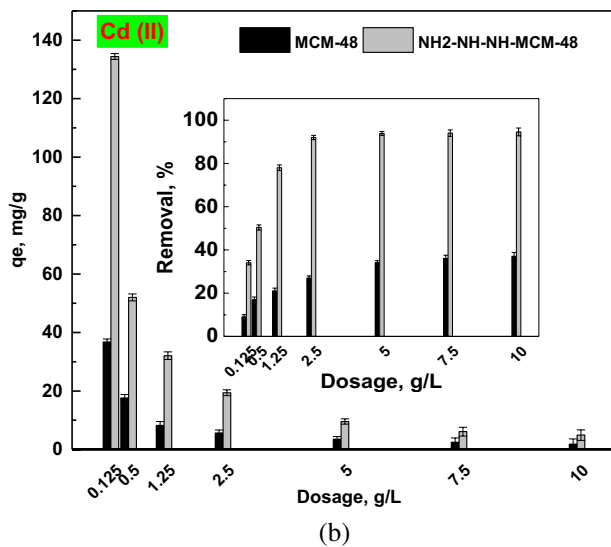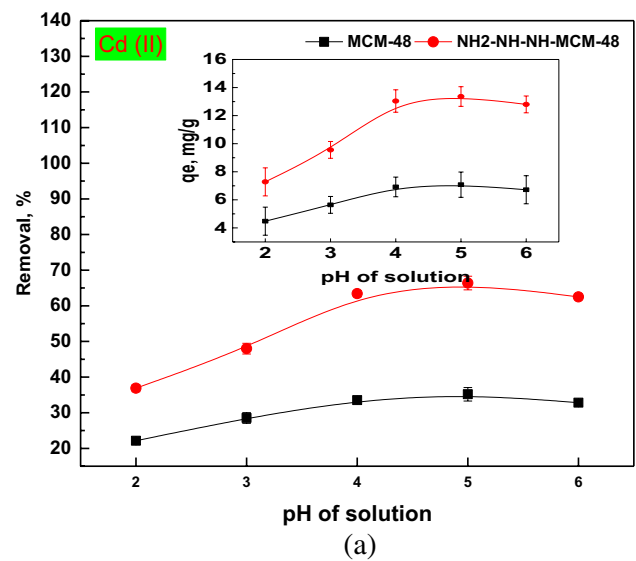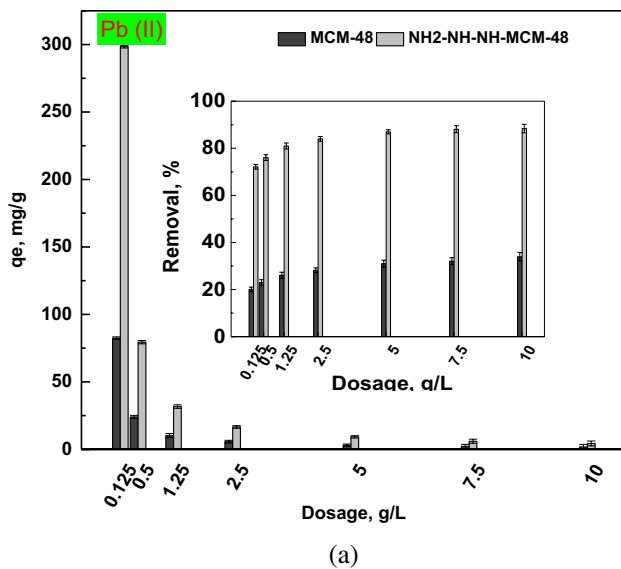
(a)

(b)

Fig. 2 Effect of adsorbent dosage of MCM-48 and NH$_2$-NH-NH-MCM-48 on the adsorption of **a** Cd (II) and **b** Pb (II) metal ions

(a)

(b)

**Fig. 3** Effect of solution pH on the adsorption of **a** Cd (II) and **b** Pb (II) metal ions with MCM-48 and NH$_2$-NH-NH-MCM-48

range was chosen because the lead precipitates at pH > 6 according to solubility rules, as examined in previous studies [30, 37, 38]. The results were presented in Fig. 3. From this graph, it was observed that as the pH of the solution increased from two to six, the adsorption capacity of Cd (II) metal ion on both adsorbents increased up to pH 5 and then decreased at pH 6. This trend was also observed for Pb (II) metal ion, while the q_m was attained at pH 4 instead of pH 5. The maximum removal of cadmium and lead ions onto MCM-48 and NH$_2$-NH-NH-MCM-48 was obtained at pH of 5 and 4, respectively.

To explain this observation, at low pH, the higher concentration and high mobility of the hydrogen ions were observed, which directly competes with the metal ions for active binding sites in the adsorbents; the overall surface charge on the adsorbent gets positive and repels the lead and cadmium cations. At a pH higher than five, the number of dominant metal ions (M) species in an aqueous solution are M(OH)$_2$. Furthermore, the low solubility of metal hydroxides results in the precipitation of metals. Thereby, the cations are not accessible to adsorb by adsorbents, reducing adsorption capacity [39, 40].

Effect of the Initial Metal Concentration

The effect of the initial Cd (II) and Pb (II) concentrations on heavy metals removal by MCM-48 and NH$_2$-NH-NH-MCM-48 was investigated from 5 to
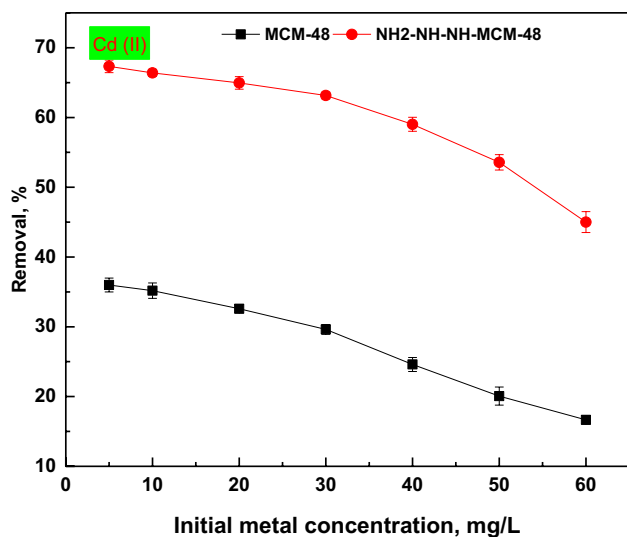
(a)
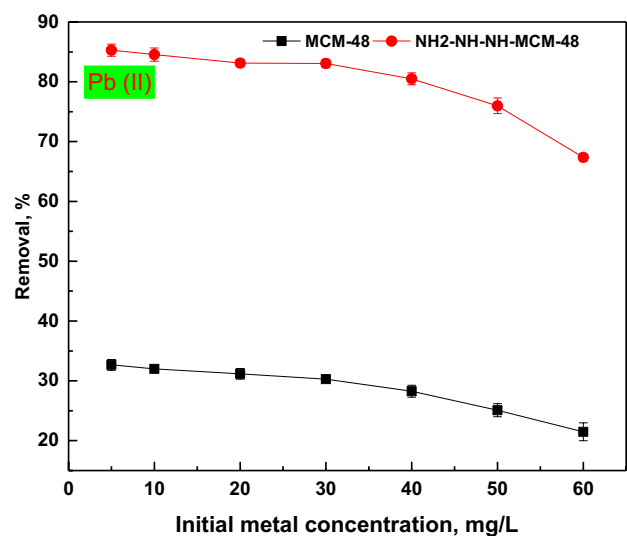
(b)

Fig. 4 Effect of initial metal concentration on the adsorption of **a** Cd (II) and **b** Pb (II) metal ions with MCM-48 and NH$_2$-NH-NH-MCM-48

(a)

(b)

Fig. 5 Langmuir, Freundlich, and Langmuir competitive adsorption isotherms of (**a** and **c**) Cd (II) and (**b** and **d**) Pb (II) onto MCM-48 and NH$_2$-NH-NH-MCM-48
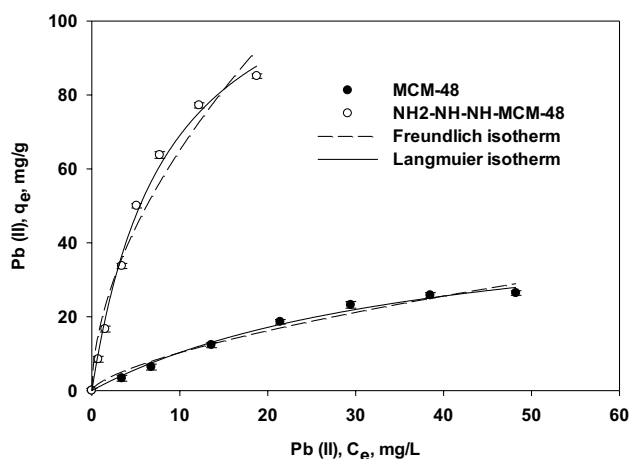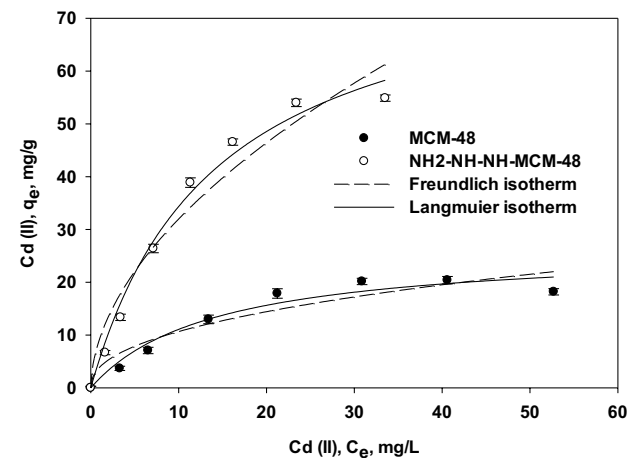
60 mg/L, and the results are depicted in Fig. 4. As seen in Fig. 4, the metal removal efficiency reduced from 39.9 to 16.6% for Cd (II) and 32.6 to 21.4% for Pb (II) in the case of MCM-48, 67.3 to 45% for Cd (II), and 85.2 to 67.3% for Pb (II) by NH2-NH-NH-MCM-48. The decrease in heavy metal ions removal efficiency with the increment of initial concentration may be ascribed to the inadequate number of active binding sites on both adsorbents. In other words, when the Pb (II) and Cd (II) concentration was increased from 5 mg/L, the MCM-48 and NH2-NH-NH-MCM-48 surface adsorption sites were saturated and unable to adsorb further metal ions, causing a reduction in metal

ions diffusion from solution to the adsorbent surface. Our findings are in agreement with Bagheri et al. [41], who prepared thiol-functionalized mesoporous silica (KIT-6-SH, MCM-41-SH, and SBA-15-SH), for the removal of Cd (II) from aqueous solution; Han et al. [16], who manufactured onto aminopropyl-functionalized MCM-48 for the removal of multi-bivalent heavy metal ions in aqueous solution; and Kenawy et al. [42], who prepared thioglycolic acid-modified mesoporous silica nanoparticles for adsorption of Cd (II) and Hg (II).

Adsorption Isotherm

The experimental adsorption data on the effect of an initial concentration of Cd (II) and Pb (II) metal ions range 10 to 50 mg L^{-1} onto MCM-48 and NH$_2$-NH-NH-MCM-48

Table 1 Adsorption parameters of the Langmuir and Freundlich isotherm models for the Cd (II) and Pb (II) adsorption onto MCM-48 and NH$_2$-NH-NH-MCM-48

Adsorbent	Metal ion	Langmuir			Freundlich			Langmuir competitive model (LCM)		
		R^2	b, l mg^{-1}	q_m, mg g^{-1}	R^2	n	K_f	R^2	b_L, l mg^{-1}	q_{mL}, mg g^{-1}
MCM-48	Cd (II)	0.982	0.060	29.13	0.942	2.09	3.50			
	Pb (II)	0.989	0.026	50.39	0.973	1.52	2.25			
NH$_2$-NH-NH-MCM-48	Cd (II)	0.988	0.071	82.70	0.954	1.86	9.28	0.992	0.055	50
	Pb (II)	0.989	0.133	119.24	0.952	1.91	19.04	0.935	0.025	73

were fitted to Langmuir and Freundlich isotherm models. The nonlinear adsorption isotherms of these models are presented in Fig. 5a and b, while the various parameters are reported in Table 1. The plot of C_e/q_e versus C_e shows that the experimental data fitted reasonably to both isotherms. The Langmuir model yields a better fit than the Freundlich model in terms of the high correlation coefficient ($R^2 > 0.98$). The q_m is estimated by the Langmuir model. For both metal ions, NH$_2$-NH-NHMCM-48 has a higher q_m than MCM-48, which was 82.7 and 119.24 mg g^{-1} for Cd (II) and Pb (II), respectively. Higher q_m and K$_L$ values for Pb (II), as compared to Cd (II), present the stronger binding affinity of MCM-48 and NH$_2$-NH-NH-MCM-48 to Pb (II) to that to Cd (II). This is attributed to the higher atomic weight, electronegativity, electrode potential, and ionic size of lead compared to cadmium [30]. The Freundlich constant (K_f and n) demonstrates whether the nature of adsorption is either favorable or unfavorable [43]. For both adsorbents, the values of n were between 1 and 10, indicating favorable adsorption.

Adsorption Kinetics

Adsorption kinetics of Cd (II) and Pb (II) metal ions uptake by NH$_2$-NH-NH-MCM-48 adsorbents were investigated based on experimental data, and the values of the constants obtained are listed in Table 2. From Table 2, it can be seen that the correlation coefficients (R^2) values of the pseudo-second-order kinetic model for all concentrations (except 60 mg L^{-1} lead) are almost higher than the R^2 values of the other models. Besides, the q_e obtained from this model were more consistent with the experimental values of adsorption capacities. Therefore, the pseudo-second-order kinetic model seemed to be an appropriate model for predicting the kinetics of Cd (II) and Pb (II) metal ions adsorption onto NH$_2$-NH-NH-MCM-48. Besides, it suggests that chemisorption occurred during the adsorption process of heavy metal ions by functionalized mesoporous silica.

Binary Adsorption of Lead and Cadmium Metals

Competitive adsorption of cadmium and lead metal ions from their binary system was examined to simulate

Table 2 Kinetic adsorption parameters obtained using pseudo-first-order and pseudo-second-order models onto NH$_2$-NH-NH-MCM-48

Metal ions	Metal cons., mg L^{-1}	q_{exp}, mg g^{-1}	Pseudo-first-order			Pseudo-second-order		
			K$_1$, min^{-1}	q_{e1}, mg g^{-1}	R^2	K$_2$	q_{e2}, mg g^{-1}	R^2
Cd (II)	5	4.92	0.009	3.08	0.903	0.016	5.14	0.990
	10	9.52	0.007	7.48	0.918	0.003	10.46	0.913
	20	18.24	0.007	14.09	0.939	0.002	19.68	0.935
	30	24.24	0.008	19.18	0.967	0.001	26.88	0.968
	40	27.92	0.010	21.94	0.962	0.001	30.86	0.974
	50	29.4	0.008	19.16	0.896	0.001	30.67	0.978
	60	30.12	0.008	28.48	0.937	0.0009	37.17	0.859
Pb (II)	5	7.22	0.010	4.53	0.906	0.011	7.58	0.982
	10	14.24	0.008	9.36	0.905	0.004	14.92	0.975
	20	27.96	0.010	20.53	0.943	0.002	30.21	0.973
	30	39.72	0.009	27.89	0.948	0.001	42.37	0.981
	40	49.28	0.008	38.07	0.931	0.0008	53.76	0.947
	50	58.4	0.010	45.40	0.973	0.0008	64.51	0.983
	60	59.92	0.010	47.44	0.972	0.0007	66.22	0.975

the actual environmental conditions where the planned application situations are complex. The LCM predicted the completive adsorption behavior of metal ions onto NH_2-NH-NH-MCM-48 with $R^2 > 0.99$ for Pb (II) and $R^2 > 0.99$ for Cd (II) metal ions. As shown in Table 1, q_m values obtained from the Langmuir model in the binary adsorption system were 50 and 73 mg g^{-1} for cadmium and lead, respectively, which were lower than those calculated in a single adsorption system. It could be attributed to interference and completion of one metal ion in adsorption of the other in a binary system.

The preference of the adsorption of a metal ion compared to another by the adsorbent in a binary system is essential. The influence of bi-solute competition on adsorption of lead and cadmium was also evaluated by using the ratio of the adsorption capacity of one metal, i, at equilibrium, in the presence of other metal, j, $q_{mL}*$, to the adsorption capacity of corresponding metal in the single metal system, q_{mL}. When the ratio $q_{mL}*$ to q_{mL} is higher than one, synergism, the adsorption is promoted by the presence of the other metal ion. For the ratio $q_{mL}*$ to q_{mL} equal to one, non-interaction, there is no apparent interaction between j and I. For the ratio $q_{mL}*$ to q_{mL} lower than 1, antagonism, the adsorption of species i is suppressed by the presence of the species j [44]. The values of maximum adsorption capacity of NH_2-NH-NH-MCM-48 for Pb (II) and Cd (II) decreased in the binary systems compared to a single system, confirming that the adsorption of these metal ions is suppressed at the presence of another metal and competitive adsorption in the binary metal systems.

Pb exhibited higher maximum adsorption capacity (73 mg g^{-1}) than Cd (50 mg g^{-1}) in binary component systems due to a more competitive ability to bind with free amine groups on the adsorbent. This could be related to the difference in metal class behavior based on the covalent index [45, 46]. The covalent index is calculated as follows [47]:

$$\text{Covalent index} = X_m^2(r + 0.85) \tag{9}$$

where X_m and r represent the electronegativity and radius of metal ion, respectively. The obtained covalent index of Pb (II) and Cd (II) was 11.8 and 5.6, respectively. According to covalent index, Pb (II) is considered a class b ion, while Cd is classified as borderline ion [45, 46]. Based on this argument, the greater the covalent index caused, the greater affinity between heavy metal ions (Pb^{2+} and Cd^{2+}) and adsorbent ligand (-NH_2 groups). As a result, Pb (II) has a higher q_m with NH_2-NH-NH-MCM-48 than Cd (II).

Table 3 Comparison of the Langmuir maximum adsorption capacity of Pb (II) and Cd (II) metal ions onto some mesoporous silica adsorbents

Adsorbents	q_{max} (mg g^{-1})		Ref
	Cd (II)	Pb (II)	
MCM-48	29.13	50.39	This study
NH_2-NH-NH-MCM-48	82.7	119.24	
NH_2-NH-NH-MCM-48[a]	50	73	
NN-MCM-48	93.4	147	[48]
Ti-MCM-48	83.57	-	[49]
N–N dimethyldodecylamine-grafted MCM-48	175.35 (1.56)[b]	238.28 (1.15)[b]	[17]
Dodecylamine-grafted MCM-48	148.38 (1.32)[b]	194.76 (0.94)[b]	
Melamine-grafted magetic-MCM-48	114.08	127.24	[50]
NH_2-MCM-41	18.25	57.74	[30]
NH_2-MCM-41	90.92	-	[51]
NH_2-MCM-48	158.7	322.6	[16]
Silica gel-aminothioamidoanthraquinone	7.53	-	[52]
MCM-41-thioglycolic acid	91.3	-	[42]
Mesoporous silica	-	9.85	[53]
SDS-MCM-41	8.61	-	[54]
Aminopropyl-MCM-41	14.08	64.21	[55]
MCM-48-NH_2	-	75.2	[56]
MCM-48-SH	-	31.2	
MDA–SBA-15	98	130.1	[57]

[a] q_m in binary system

[b] mmol/g

Table 4 Desorption of Cd (II) and Pb (II) metal ions by MCM-48 and NH$_2$-NH-NH-MCM-48

Metal ion	Adsorbent	Parameter	Number of cycles				
			#1	#2	#3	#4	#5
Cd (II)	MCM-48	R, (%)	35.30	29.19	25.84	20.71	13.61
		q_e, (mg g^{-1})	7.16	5.92	5.24	4.2	2.76
	NH$_2$NHNH-MCM-48	R, (%)	66.69	62.15	56.71	49.20	37.54
		q_e, (mg g^{-1})	13.5	12.58	11.48	9.96	7.6
Pb (II)	MCM-48	R, (%)	32.07	28.88	22.71	19.12	16.13
		q_e, (mg g^{-1})	6.44	5.80	4.56	3.84	3.24
	NH$_2$NHNH-MCM-48	R, (%)	84.47	79.43	75.00	68.54	61.89
		q_e, (mg g^{-1})	16.76	15.76	14.88	13.60	12.28

Comparison with Other Adsorbents

Table 3 shows the values of Langmuir adsorption capacity (q_m) for the adsorption of Cd (II) and Pb (II) on different mesoporous silica adsorbents reported in the literature. As shown in Table 3, Chen et al. [49] prepared Ti-MCM-48 for adsorption of Cd (II) cation and the obtained q_m was 83.5 mg g^{-1} which was near the q_m acquired in this study (82.7 mg g^{-1}). The adsorption capacity of mesopressure silica is influenced by two factors: (1) type of mesoporous silicate and (2) density of the amine groups bonded to silica [20, 58, 59]. Faghihian and Naghavi functionalized MCM-48 with amino-ethylamino]-propyltrimethoxysilane (NN-MCM-48). The obtained values of q_m were 93.4 and 147 mg g^{-1} for Cd and Pb, respectively. The q_m for Cd and Pb with NNN-MCM-48 in this study were 82.7 and 119.2 mg g^{-1}, respectively. This reduction in adsorption capacity is probably due to the low density of amine groups in the mesoporous structure. This is in agreement with the Yokoi et al. [20] findings. They modified MCM-41 with mono-, di-, and tri-amino-organoalkoxysilanes and used it for heavy metal adsorption. Their results indicated that the q_m was improved with increment in the density of amino functional groups. Moreover, the adsorption capacities of heavy metals decreased when NNN silane was grafted to the mesoporous surface. Furthermore, the q_m reported by Benhamou et al. [17] for Cd (II) and Pb (II) cations using N–N dimethyldodecylamine- and dodecylamine-grafted MCM-48 and those obtained by Aniba et al. [50] with magnetic mesoporous silica MCM-48 modified with melamine-based dendrimer amine were higher than those in this research. The reason for the high q_m in these studies can be associated with other factors such as the availability of amine groups and branched chain of amine group in a mesoporous structure that have a positive effect on adsorption [60, 61]. Besides, other members of the mesoporous silica family, such as amine-grafted MCM-41 and SBA-15, showed higher q_m for Cd and Pb due to having different pore sizes and surface area. Da'na [59] found that silica structural order, pore size, and surface area are significant mesoporous material parameters to determine their affinity to adsorption heavy metal ions.

Desorption Study

Desorption of lead and cadmium metal ions from MCM-48 and NH$_2$-NH-NH-MCM-48 using HNO$_3$ as a desorbing agent into desorption medium was investigated. The results related to removing the number of ions desorbed and adsorption capacity after five successive adsorption–desorption cycles are shown in Table 4. As can be seen from Table 4, the dominant part of the metal was removed in the first desorption cycle and HNO$_3$ was efficient in desorbing the metal ions, especially NH$_2$-NH-NH-MCM-48. For example, the desorption efficiency of Pb (II) metal ion by this adsorbent was about 84.5% in the first cycle, and in 2, 3, 4, and 5 cycles were 79.4, 75, 68.6, and 61.9%, respectively. For MCM-48, at the first cycle, the obtained maximum removal was 35.3 and 32% for cadmium and lead, respectively, and it decreased at subsequent cycles. Furthermore, the re-adsorption results of Cd (II) and Pb (II) ions using both the spent adsorbents demonstrate that the adsorbents could be reused up to 5 times but their adsorption capacity decreased but this reduction was not significant for NH2NHNH-MCM-48 adsorbent.

Conclusion

The efficiency of MCM-48 and amine-functionalized MCM-48 (NH$_2$-NH-NH-MCM-48) for the competitive adsorption of cadmium and lead was examined. The characteristics of these adsorbents were determined by XRD, SEM, and N$_2$ adsorption–desorption. The batch experimental adsorption was conducted in single and binary systems and the effects of adsorbent dosage, pH, contact time, and initial metal concentrations were studied. With both adsorbents, the optimal pH for removal of cadmium and lead was 5 and 4, respectively. The Langmuir and Freundlich isotherm models

were fitted with the adsorption experimental data, and the Langmuir equation indicated a better fit than the Freundlich model, in terms of the higher correlation coefficients. According to the Langmuir model, for both metal ions, NH_2-NH-NHMCM-48 has a higher maximum adsorption capacity than MCM-48, which was 82.7 and 119.24 mg g^{-1} for cadmium and lead, respectively. The binary metal mixture adsorption results confirm that the adsorption of these metal ions is suppressed in the metal's presence. The two-component equilibrium data were fitted to the modified, extended Langmuir.

Authors' Contribution All authors have participated in the (a) conception and design, or analysis and interpretation of the data; (b) drafting the article or revising it critically for important intellectual content; and (c) approval of the final version.

Declarations

This manuscript has not been submitted to, nor is under review at, another journal or other publishing venue.
The authors have no affiliation with any organization with a direct or indirect financial interest in the subject matter discussed in the manuscript.

Conflict of Interest The authors declare no competing interests.

References

1. Wang J, Chen C (2006) Biosorption of heavy metals by Saccharomyces cerevisiae: a review. Biotechnol Adv 24:427–451
2. Bahadir T, Bakan G, Altas L, Buyukgungor H (2007) The investigation of lead removal by biosorption: an application at storage battery industry wastewaters. Enzyme Microb Technol 41:98–102
3. Medellin-Castillo NA, Padilla-Ortega E, Regules-Martínez MC, Leyva-Ramos R, Ocampo-Pérez R, Carranza-Alvarez C (2017) Single and competitive adsorption of Cd(II) and Pb(II) ions from aqueous solutions onto industrial chili seeds (Capsicum annuum) waste. Sustain Environ Res 27:61–69
4. Ding Z, Hu X, Morales VL, Gao B (2014) Filtration and transport of heavy metals in graphene oxide enabled sand columns. Chem Eng J 257:248–252
5. Petrinic I, Korenak J, Povodnik D, Hélix-Nielsen C (2015) A feasibility study of ultrafiltration/reverse osmosis (UF/RO)-based wastewater treatment and reuse in the metal finishing industry. J Clean Prod 101:292–300
6. Zewail TM, Yousef NS (2015) Kinetic study of heavy metal ions removal by ion exchange in batch conical air spouted bed. Alex Eng J 54:83–90
7. Bailliez S, Nzihou A, Bèche E, Flamant G (2004) Removal of Lead (Pb) by Hydroxyapatite Sorbent. Process Saf Environ Prot 82:175–180
8. Mohamed Belmedani HH, Sadaoui Z (2009) Removal of cadmium from aqueous solutions by adsorption onto activated carbon prepared from date stems. 15th International Conference on Heavy Metals in the Environment, Poland
9. Robles I, Bustos E, Lakatos J (2016) Adsorption study of mercury on lignite in the presence of different anions. Sustain Environ Res 26:136–141
10. Hosseini R, Sayadi MH, Shekari H (2019) Adsorption of nickel and chromium from aqueous solutions using copper oxide nanoparticles: Adsorption isotherms, kinetic modeling, and thermodynamic studies. Avicenna J Environ Health Eng 6:66–74
11. Sayadi MH, Rashki O, Shahri E (2019) Application of modified Spirulina platensis and Chlorella vulgaris powder on the adsorption of heavy metals from aqueous solutions. J Environ Chem Eng 7:103169
12. Chang JC, Ko AN (2004) Novel synthesis of [var epsilon]-caprolactam from cyclohexanone-oxime via Beckmann rearrangement over mesoporous molecular sieves MCM-48. Catal Today 97:241–7
13. Srisuda S, Virote B (2008) Adsorption of formaldehyde vapor by amine-functionalized mesoporous silica materials. J Environ Sci 20:379–84
14. Beck JS, Vartuli JC, Roth WJ, Leonowicz ME, Kresge CT, Schmitt KD, Chu CTW, Olson DH, Sheppard EW (1992) A new family of mesoporous molecular sieves prepared with liquid crystal templates. J Am Chem Soc 114:10834–43
15. Zadeh RJ, Sayadi MH, Rezaei MR (2021) Synthesis of Thiol modified magMCM-41 nanoparticles with rice husk ash as a robust, high effective, and recycling magnetic sorbent for the removal of herbicides. J Environ Chem Eng 9:104804
16. Han Y, Chen J, Gu X, Chen J (2020) Adsorption of multi-bivalent heavy metal ions in aqueous solution onto aminopropyl-functionalized MCM-48 preparation by co-condensation. Sep Sci Technol 1–11
17. Benhamou A, Baudu M, Derriche Z, Basly JP (2009) Aqueous heavy metals removal on amine-functionalized Si-MCM-41 and Si-MCM-48. J Hazard Mater 171:1001–1008
18. Ebrahimzadeh H, Tavassoli N, Amini M, Fazaeli Y, Abedi H (2010) Determination of very low levels of gold and palladium in wastewater and soil samples by atomic absorption after preconcentration on modified MCM-48 and MCM-41 silica. Talanta 81:1183–1188
19. Wang X-J, Xia S-Q, Chen L, Zhao J-F, Chovelon J-M, Nicole J-R (2006) Biosorption of cadmium(II) and lead(II) ions from aqueous solutions onto dried activated sludge. J Environ Sci 18:840–4
20. Yokoi T, Yoshitake H, Tatsumi T (2004) Synthesis of amino-functionalized MCM-41 via direct co-condensation and post-synthesis grafting methods using mono-, di- and tri-amino-organoalkoxysilanes. J Mater Chem 14:951–957
21. Rozada F, Otero M, García AI, Morán A (2007) Application in fixed-bed systems of adsorbents obtained from sewage sludge and discarded tyres. Dyes Pigm 72:47–56
22. Park Y, Sin WS, Choi SJ (2012) Removal of Co, Sr and Cs from aqueous solution using self-assembled monolayers on mesoporous supports. Korean J Chem Eng 29:1556–66
23. Sdiri AT, Higashi T, Jamoussi F (2014) Adsorption of copper and zinc onto natural clay in single and binary systems. Int J Environ Sci Technol (Tehran) 11:1081–1092
24. Sdiri AHT (2013) Simultaneous removal of heavy metals from aqueous solution by natural limestones. Appl Water Sci 3:29–39
25. Srivastava VC, Mall ID, Mishra IM (2009) Equilibrium Modeling of Ternary Adsorption of Metal Ions onto Rice Husk Ash. J Chem Eng Data 54:705–711
26. Yu J-X, Wang L-Y, Chi R-A, Zhang Y-F, Xu Z-G, Guo J (2013) Competitive adsorption of Pb2+ and Cd2+ on magnetic modified sugarcane bagasse prepared by two simple steps. Appl Surf Sci 268:163–170
27. Ding P, Huang K-L, Li G-Y, Zeng W-W (2007) Mechanisms and kinetics of chelating reaction between novel chitosan derivatives and Zn(II). J Hazard Mater 146:58–64
28. Lagergren S (1898) About the theory of the so-called adsorption of soluble substances. Kungliga SvenskaVetenskapsakademius, Hadndlingar 24:1–39

29. Ho YS, Mckay G (1998) 1998, 16, Kinetic model for lead (II) sorption on peat. Adsorpt Sci Technol 16:243–255

30. Heidari A, Younesi H, Mehraban Z (2009) Removal of Ni(II), Cd(II), and Pb(II) from a ternary aqueous solution by amino functionalized mesoporous and nano mesoporous silica. Chem Eng J 153:70–79

31. Puanngam M, Unob F (2008) Preparation and use of chemically modified MCM-41 and silica gel as selective adsorbents for Hg(II) ions. J Hazard Mater 154:578–587

32. Fei Z, Ai S, Zhou Z, Chen X, Tang J, Cui M et al (2014) Enhanced activity of MCM-48 based tin catalyst for synthesis of 3-methylbut-3-en-1-ol by adjusting the mesochannel environment. J Ind Eng Chem 20:4146–4151

33. Wu J, Song Y, Han B, Wei J, Wei Z, Yang Y (2015) Synthesis and characterization of UV upconversion material Y2SiO5:Pr3+, Li+/TiO2 with enhanced the photocatalytic properties under a xenon lamp. RSC Adv 5:49356–49362

34. Castruita-de León G, Perera-Mercado YA, García-Cerda LA, Mercado-Silva JA, Meléndez-Ortiz HI, Olivares-Maldonado Y et al (2015) Synthesis of amino-functionalized MCM-48 silica via direct co-condensation at room temperature. Microporous Mesoporous Mater 204:156–162

35. Huang HY, Yang RT, Chinn D, Munson CL (2003) Amine-Grafted MCM-48 and Silica Xerogel as Superior Sorbents for Acidic Gas Removal from Natural Gas. Ind Eng Chem Res 42:2427–2433

36. Anbia M, Kargosha K, Khoshbooei S (2015) Heavy metal ions removal from aqueous media by modified magnetic mesoporous silica MCM-48. Chem Eng Res Des 93:779–788

37. Tunali S, Çabuk A, Akar T (2006) Removal of lead and copper ions from aqueous solutions by bacterial strain isolated from soil. Chem Eng J 115:203–211

38. Chang J-S, Law R, Chang C-C (1997) Biosorption of lead, copper and cadmium by biomass of Pseudomonas aeruginosa PU21. Water Res 31:1651–1658

39. Mehdizadeh S, Sadjadi S, Ahmadi SJ, Outokesh M (2014) Removal of heavy metals from aqueous solution using platinum nanopartcles/Zeolite-4A. J Environ Health Sci Eng 12:1–7

40. Bouhamed F, Elouear Z, Bouzid J (2012) Adsorptive removal of copper(II) from aqueous solutions on activated carbon prepared from Tunisian date stones: Equilibrium, kinetics and thermodynamics. J Taiwan Inst Chem Eng 43:741–749

41. Bagheri S, Amini MM, Behbahani M, Rabiee G (2019) Low cost thiol-functionalized mesoporous silica, KIT-6-SH, as a useful adsorbent for cadmium ions removal: a study on the adsorption isotherms and kinetics of KIT-6-SH. Microchem J 145:460–469

42. Kenawy IMM, Abou El-Reash YG, Hassanien MM, Alnagar NR, Mortada WI (2018) Use of microwave irradiation for modification of mesoporous silica nanoparticles by thioglycolic acid for removal of cadmium and mercury. Microporous Mesoporous Mater 258:217–227

43. Frimmel FH, Huber L (1996) Influence of humic substances on the aquatic adsorption of heavy metals on defined mineral phases. Environ Int 22:507–517

44. Ronda A, Martín-Lara MA, Dionisio E, Blázquez G, Calero M (2013) Effect of lead in biosorption of copper by almond shell. J Taiwan Inst Chem Eng 44:466–473

45. Xu W, Lan H, Wang H, Liu H, Qu J (2015) Comparing the adsorption behaviors of Cd, Cu and Pb from water onto Fe-Mn binary oxide, MnO2 and FeOOH. Front Environ Sci Eng 9:385–393

46. Iqbal M, Edyvean RGJ (2004) Biosorption of lead, copper and zinc ions on loofa sponge immobilized biomass of Phanerochaete chrysosporium. Miner Eng 17:217–223

47. Nieboer E, McBryde WAE (1973) Free-energy Relationships in Coordination Chemistry. III. A Comprehensive Index to Complex Stability. Can J Chem 51:2512–24

48. Faghihian H, Naghavi M (2014) Synthesis of amine-functionalized MCM-41 and MCM-48 for removal of heavy metal ions from aqueous solutions. Sep Sci Technol 49:214–220

49. Chen J, Fang K, Wu L, Qian Z, Chen J (2011) Removal of Cd(II) from Aqueous by Adsorption onto Mesoporous Ti-MCM-48. Procedia Environ Sci 10(Part C):2491–7

50. Anbia M, Khoshbooei S (2015) Functionalized magnetic MCM-48 nanoporous silica by cyanuric chloride for removal of chlorophenol and bromophenol from aqueous media. J Nanostruct Chem 5:139–146

51. Ghrobani F, Younesi H, Mehraban Z, Sabri Celik M, Ghoreyshi AA, Anbia M (2013) Aqueous cadmium ions removal by adsorption on APTMS grafted meso porous silica MCM-41 in batch and fixed bed column processes. Int J Eng 26:473–488

52. Ngeontae W, Aeungmaitrepirom W, Tuntulani T (2007) Chemically modified silica gel with aminothioamidoanthraquinone for solid phase extraction and preconcentration of Pb (II), Cu (II), Ni (II), Co (II) and Cd (II). Talanta 71:1075–1082

53. Lin L-C, Thirumavalavan M, Wang Y-T, Lee J-F (2010) Surface area and pore size tailoring of mesoporous silica materials by different hydrothermal treatments and adsorption of heavy metal ions. Colloids Surf Physicochem Eng Aspects 369:223–231

54. Kaewprachum W, Wongsakulphasatch S, Kiatkittipong W, Striolo A, Cheng CK, Assabumrungrat S (2020) SDS modified mesoporous silica MCM-41 for the adsorption of Cu2+, Cd2+, Zn2+ from aqueous systems. J Environ Chem Eng 8:102920

55. Du Dinh P, Hieu NT, To TC, Bach LG, Tinh MX, Xuan Mau T et al (2019) Aminopropyl Functionalised MCM-41: Synthesis and Application for Adsorption of Pb(II) and Cd(II). Adv Mater Sci Eng 2019:8573451

56. Malhis AA, Arar SH, Fayyad MK, Hodali HA (2018) Amino-and thiol-modified microporous silicalite-1 and mesoporous MCM-48 materials as potential effective adsorbents for Pb (II) in polluted aquatic systems. Adsorpt Sci Technol 36:270–286

57. Shahbazi A, Younesi H, Badiei A (2011) Functionalized SBA-15 mesoporous silica by melamine-based dendrimer amines for adsorptive characteristics of Pb(II), Cu(II) and Cd(II) heavy metal ions in batch and fixed bed column. Chem Eng J 168:505–518

58. Melero JA, van Grieken R, Morales G (2006) Advances in the synthesis and catalytic applications of organosulfonic-functionalized mesostructured materials. Chem Rev 106:3790–3812

59. Da'na E (2017) Adsorption of heavy metals on functionalized-mesoporous silica: a review. Microporous Mesoporous Mater 247:145–157

60. Bhagiyalakshmi M, Yun LJ, Anuradha R, Jang HT (2010) Utilization of rice husk ash as silica source for the synthesis of mesoporous silicas and their application to CO2 adsorption through TREN/TEPA grafting. J Hazard Mater 175:928–938

61. Kim S, Ida J, Guliants VV, Lin YS (2005) Tailoring pore properties of MCM-48 silica for selective adsorption of CO2. J Phys Chem B 109:6287–6293